Animal Models of Diabetic Complications Consortium (U01 DK076160)

Annual Report (2008)

Mitochondrial SOD as a Target for Diabetic Neuropathy

Eva L. Feldman, M.D., Ph.D.

Eva L. Feldman, M.D., Ph.D.
University of Michigan
Department of Neurology
Ann Arbor, MI 48109-2200
Phone: (734) 763-7274 Fax: (734)763-7275
Email: efeldman@umich.edu

Table of Contents

Animal Models of Diabetic Complications Consortium

U01 DK07160

Part A:

Principal Investigator's Summary

1. Program Accomplishments:

Rodent models of diabetes fail to develop changes that closely resemble human diabetic nephropathy or neuropathy. While the reasons for the resistance of rodents to full-blown complications are likely multiple, they may include an increased resistance to oxidative stress or the absence of important genetic susceptibility genes. Our general strategic approach to this dilemma is to accelerate the injury of diabetes by predisposing critical cells within the peripheral nervous system to glucose-mediated oxidative injury.

Recent Progress and Major Accomplishments

Thiazolidinediones (TZDs) are potent insulin sensitizers used to treat type 2 diabetes and insulin resistant type 1 diabetes (1). TZDs were first identified as insulin sensitizing agents by Chang et al (2, 3) and Fujita et al (4), who evaluated their antidiabetic effects in mouse models of type 2 diabetes and a rat model of type 1 diabetes. The mechanism of this antidiabetic activity was determined to be activation of PPAR-gamma, a transcription factor in the nuclear receptor family (5). While other PPAR transcription factors are ubiquitously expressed, PPAR-gamma is specific to adipose tissue, kidney, liver and Schwann cells (6, 7). Microarray studies of gene regulation by TZDs found that they alter steady state mRNA levels of several hundred genes, primarily those involved in glucose and lipid metabolism (8).

Recent evidence suggests that TZDs reduce the development of diabetic complications independent of insulin sensitization. TZD treatment reduces the formation of atherosclerotic plaques (9), a macrovascular complication, and also reduces oxidative stress and the inflammatory response (10), two mechanisms of microvascular complications. TZD effects on oxidative stress are attributable to a number of potential causes, including altered expression of NADPH oxidase and improvement of mitochondrial health (11, 12). Two studies were performed demonstrating that TZDs slow or prevent the development of diabetic neuropathy (DN) in models of type 1 diabetes. In streptozotocin (STZ)-treated rats, troglitazone protects against nerve conduction velocity slowing, and maintains normal myelinated fiber architecture and number (13). Pioglitizone also has neuroprotective effects on nerve conduction velocity and reduces macrophage infiltration in the sciatic nerve (6). These improvements in the DN profile of the diabetic rats can not be explained by insulin sensitization, and are due to some other effect of TZDs. Troglitazone is an innate antioxidant as well as a glitizone (14), and may reduce oxidative stress independent of transcription factor activation. No such alternative mechanism is known for pioglitizone, and changes in protein expression suggest that a gene regulatory mechanism was activated (9). A systems biology approach may elucidate this gene regulatory mechanism, but a rat model of diabetes was used by both research groups, which is non-ideal for gene expression profiling.

While TZDs have significant promise in the treatment of DN, their side effects may limit their usefulness (15-17). Due to the heterogeneous complications of members of the TZD family, we hypothesize that the beneficial effects of TZDs on diabetic complications are independent of the mechanisms that cause adverse effects. Screening the gene expression patterns induced in the nerve by PPAR-gamma agonist activity may allow us to separate these positive and negative effects and identify regulatory mechanisms that affect development of DN. We examined changes in gene expression in sciatic nerves of mice with STZ induced diabetes and TZD treatment to define downstream transcriptional responses. Using systems biology, we inferred likely regulatory mechanisms based on those changes. Such regulatory mechanisms constitute starting points for more specific drug target development with the potential to separate the beneficial and harmful effects of TZDs. A TZD with no known innate antioxidant capacity, Rosiglitazone (Rosi), was chosen as the treatment to minimize the potential confounding effects

on oxidative stress. Gene expression changes were measured using Affymetrix microarrays, revealing novel transcriptional control sequences are present in genes strongly correlated with DN.

Induction of Diabetes and Rosi Treatment

DBA/2J mice (Stock Number: 000671) were purchased from Jackson Laboratories (Bar Harbor, Maine). Breeding colonies established at the University of Michigan provided the animals used in this study. Mice were housed in a pathogen-free environment, and cared for following the University of Michigan Committee on the Care and Use of Animals guidelines. Mice were fed powdered mouse chow (Purina 5001).

Four treatment groups were defined: control (n = 17), diabetic (n = 15), control + Rosi (n = 18) and diabetic + Rosi (n = 13). Diabetes was induced by low-dose STZ treatment (50 mg/kg for 5 days) when the animals reached a weight of 22 g (~ 10 weeks old). Two weeks after STZ treatment, or the equivalent time point for Control mice, Rosi (3 mg/kg po/day) was given in Nutra-Cal (EVSCO Pharmaceuticals, Buena, NJ) to half of the diabetic and control animals. To increase survival, diabetic and diabetic + Rosi mice were implanted with a sustained release insulin implant (Linbit for mice 0.1 U insulin/day/implant, LINSHIN Canada, Inc) 15 weeks post-STZ treatment. A second implant was inserted following 20 weeks of diabetes.

Animals were phenotyped for diabetes, measures of oxidative stress and DN per our published protocols (18, 19).

Fasting Blood Glucose, GHb

Fasting blood glucose was significantly elevated in diabetic mice 6, 12, 16, 20 & 24 weeks post-STZ ($p < 0.001$). GHb was also significantly increased after 24 weeks, indicative of prolonged hyperglycemia ($p < 0.001$). Diabetic mice lost a significant amount of weight compared to control mice ($p < 0.001$). Rosi treatment had no significant effect on blood glucose, GHb, or weight loss in the DBA/2J mice (Table 1). There is no evidence that the levels of insulin provided to the mice resolved their diabetes or that Rosi treatment enhanced the efficacy of the insulin supplement.

Table 1 - Metabolic Parameters of the DBA/2J Mice.

Glycemic Status	Treatment	Final Weight	Final Blood Glucose	GHb
Nondiabetic	None	29.7 ± 3.9, *n = 17*	122.1 ± 18.5, *n = 17*	5.8 ± 0.9, *n = 15*
Diabetic	STZ	23.5 ± 1.7, *n = 18*	455.2 ± 163.6, *n = 18*	14.2 ± 1.7, *n = 18*
Nondiabetic	Rosi	29.2 ± 3.2, *n = 15*	122.8 ± 16.3, *n = 15*	6.0 ± 0.7, *n = 15*
Diabetic	STZ & Rosi	23.7 ± 1.5, *n = 13*	509 ± 153.5, *n = 13*	13.6 ± 2.0, *n = 13*

Final weight was reduced in diabetic mice ($p < 0.001$); final blood glucose and GHb were increased ($p < 0.001$).

Neuropathy

DN in the DBA/2J mice was assessed by thermal latency in the hind paw and nerve conduction velocity (NCV) in the sciatic and sural nerves. Thermal latency was significantly increased following 24 weeks of diabetes (control = 6.3 ± 1.0 s, diabetic = 11.1 ± 0.8 s, $p < 0.001$, Fig. 1). Despite maintaining the same mean blood glucose as diabetic mice (Table 1), the diabetic + Rosi mice had significantly lower thermal latency (diabetic + Rosi = 7.6 ± 1.2, $p < 0.001$). Sensory and motor NCV were measured in the sural and sciatic nerves. Sural NCV was decreased by 14% in diabetic mice (control = 23.7 ± 3.5 m/sec, diabetic = 20.3 ± 3.2 m/sec, $p < 0.05$), while sciatic NCV was decreased by 24% in diabetic mice (control = 45.5 ± 3.9 m/sec, diabetic = 34.4 ± 7.1 m/sec, $p < 0.01$). While there was a trend toward reduced impairment of NCV following Rosi treatment, it did not reach significance.

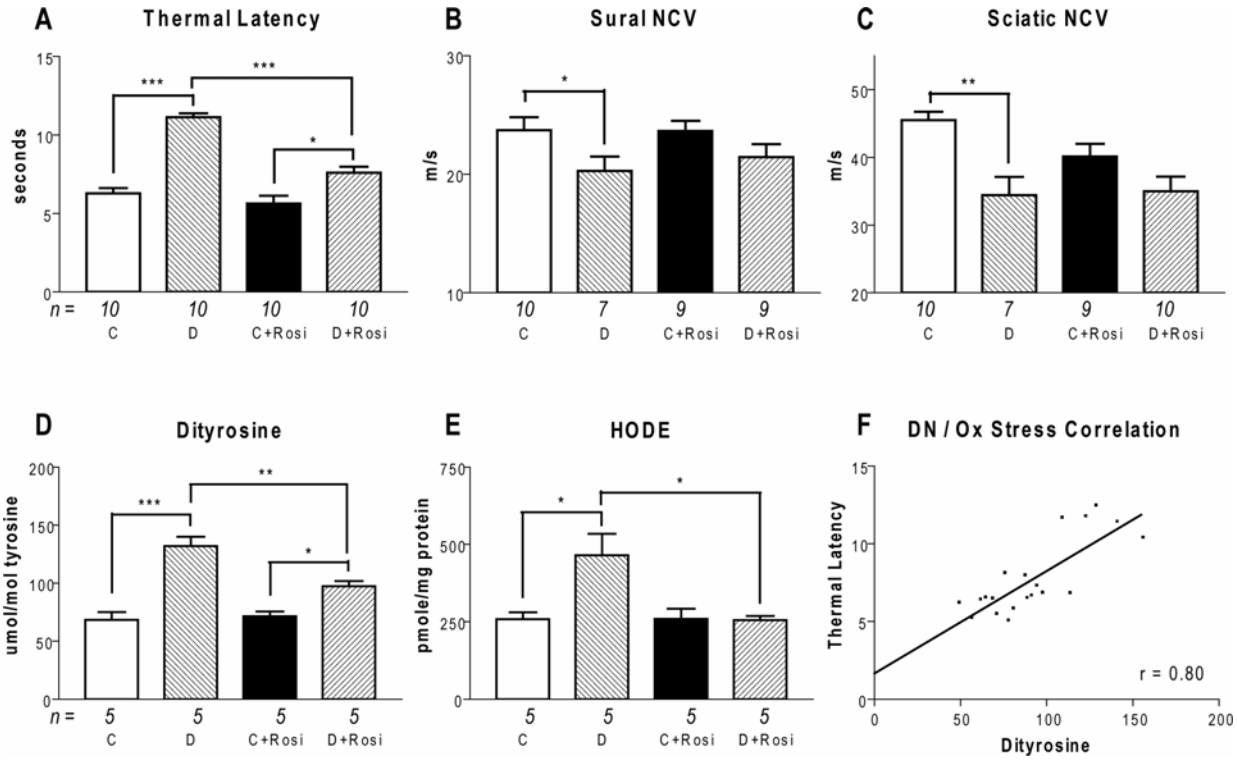

Fig. 1. DN and Oxidative Stress Measures. A) Hind paw withdrawal latency was increased in diabetic mice and reduced by Rosi treatment. B) Sural sensory NCV was reduced in diabetic mice. C) Sciatic motor NCV was reduced in diabetic mice. Hind paw latency, sural sensory NCV, and sciatic motor NCV were not affected by Rosi treatment in control mice (C, C + Rosi). D) The dityrosine/tyrosine ratio was increased in diabetic mice, and reduced by Rosi treatment. Dityrosine was still increased in diabetic mice treated with Rosi compared with control mice treated with Rosi. E) HODE was increased in diabetic mice and decreased by Rosi treatment. There was no difference between control and diabetic mice treated with Rosi. F) There is a significant correlation between thermal latency and dityrosine ratio. * $p < 0.05$, ** $p < 0.01$, *** $p < 0.001$.

Oxidative Stress Measures

Oxidative stress is a major mechanism of hyperglycemia-induced DN in humans, particularly through the oxidation of proteins and lipids. To determine whether oxidative stress was elevated in the DBA/2J-STZ mice, we quantified levels of protein-bound O,O'-dityrosine and

Hydroxyoctadecadienoic acids (HODE) in the nerve. Dityrosine was significantly increased by diabetes (control = 68.4 ± 15.0 umol/mol tyrosine, diabetic = 131.9 ± 17.9 umol/mol, $p < 0.001$). This effect was reduced significantly by treatment with Rosi (diabetic + Rosi = 97.3 ± 10.1 umol/mol, $p < 0.01$). HODE in the nerve was also significantly increased by diabetes (control = 259.2 ± 47.4 pmole/mg protein, diabetic = 465.4 ± 154.7 pmole/mg, $p < 0.05$) and the effect was attenuated by Rosi (diabetic + Rosi = 255.2 ± 31.1 pmole/mg, $p < 0.05$). Rosi treatment did not affect dityrosine or HODE in non-diabetic DBA/2J mice.

The correlation between thermal latency and dityrosine was found to be highly significant ($r = 0.80$, $p < 0.001$), as was the correlation between thermal latency and HODE ($r = 0.71$, $p < 0.001$). We hypothesized that Rosi activates cellular mechanisms of free radical management. We tested this hypothesis by analyzing gene expression patterns in DBA/2J mice.

Gene Expression Changes in Diabetes

Affymetrix Mouse Genome 430 2.0 microarrays were used to measure the expression of 12,150 genes in the sciatic nerve (n = 5 mice per group). One array of a control animal did not pass quality control and was excluded from further analysis (data not shown). Changes in expression between groups were tested by a t-test and the CyberT false discovery rate (FDR) (20). Genes with both a p-value and FDR below 0.05 were considered differentially regulated genes (DEG). A total of 526 DEGs were found between control and diabetic, 318 between diabetic and diabetic + Rosi, and 345 between control and control + Rosi. The DEGs between control and diabetic mice were clustered into functional categories using the DAVID functional annotation tool (Table 2). Some diabetic DEGs were also significantly regulated by Rosi treatment. Fifteen genes were down-regulated by diabetes and up-regulated by Rosi and 68 up-regulated by diabetes and down-regulated by Rosi (Fig. 2A & B). Eight genes regulated by diabetes and Rosi were validated by quantitative real time RT-PCR (Table 3). While changes in expression did not consistently reach significance, the trend of down-regulation in diabetes and partial normalization with Rosi treatment was confirmed in 4 out of 8 genes (Fig. 2C).

Table 2 - DAVID Enrichment Categories.

Overall Function	Median Enrichment p-value
Metabolism	3.75×10^{-5}
Metal Ion Binding	9.57×10^{-4}
mRNA Processing	3.60×10^{-4}
Cellular Regulation	7.75×10^{-3}
Mitochondria & Energy Production	1.25×10^{-2}

Genes significantly regulated in diabetes relative to control were analyzed with the DAVID Functional Annotation Clustering. The table lists the top 5 non-redundant functional clusters and the median p-value of each member of the cluster. The enrichment p-value is the probability of finding as many regulated genes in a functional category as were observed, calculated using Fisher's Exact Test. Because DAVID clusters annotation from over 40 different sources (including GO, KEGG, Swiss-prot), the median p-value from each cluster was used to rank its relative significance.

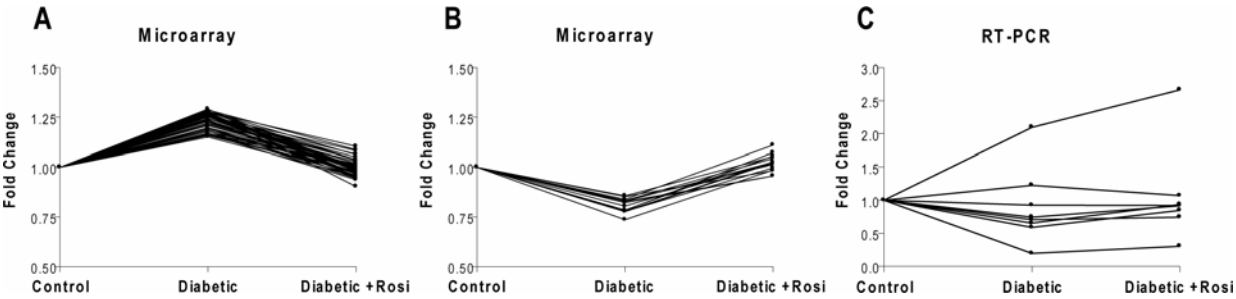

Fig. 2. Patterns of Gene Regulation. Each line is the Fold Change v. Control of one gene across the three different conditions. Genes regulated by both diabetes and Rosi were found to either A) increase with diabetes and decrease with Rosi treatment or B) decrease in expression in diabetes and increase with Rosi treatment. C) The gene expression pattern of eight genes down-regulated by diabetes and up-regulated by Rosi was confirmed by real-time RT-PCR.

Table 3 – Genes Tested by RT-PCR

Gene ID	Gene Name	Correlation
99543	olfactomedin-like 3	0.960348
228357	low density lipoprotein receptor-related protein 4	0.864936
94249	solute carrier family 24 (sodium/potassium/calcium exchanger), member 3	0.706296
17183	matrilin 4	0.683156
11865	aryl hydrocarbon receptor nuclear translocator-like	0.374882
14194	fumarate hydratase 1	0.353724
192650	calcium binding protein 7	-0.40936
56758	muscleblind-like 1 (Drosophila)	-0.92576

Gene ID is the EntrezGene accession number that uniquely identifies the gene. Correlation is between the expression level of each gene as measured by the Affymetrix chip and RT-PCR.

Promoter Module Enrichment

Groups of functionally related genes regulated in the same direction by diabetes may be under the control of conserved transcription factor (TF) binding modules. TFs bind to specific DNA sequences called motifs. Two or more motifs arranged in a consistent order with a consistent spacing in the promoter sequence are designated a TF binding module. Such modules are core features of translation initiation sites. The genes regulated by diabetes identified as either metabolic or mitochondrial by the DAVID functional annotation tool (Table 4) were separated into up- and down-regulated genes (Table 4).

Table 4 – Significantly Regulated Genes Related to Mitochondrial Function and Metabolism.

Gene ID	Gene Name	Fold Change
18746	pyruvate kinase, muscle	1.64
18618	phosphatidylethanolamine N-methyltransferase	1.43
67681	mitochondrial ribosomal protein L18	1.43
67582	solute carrier family 25 (mitochondrial carrier, phosphate carrier), member 26	1.42
12856	cytochrome c oxidase, subunit XVII assembly protein homolog (yeast)	1.36
20655	superoxide dismutase 1, soluble	1.35
14467	glioblastoma amplified sequence	1.34
22262	urate oxidase	1.33
28030	G elongation factor, mitochondrial 1	1.32
68375	NADH dehydrogenase (ubiquinone) 1 alpha subcomplex, 8	1.29
66988	leucine aminopeptidase 3	1.29
13171	dihydrolipoamide branched chain transacylase E2	1.28
50776	polymerase (DNA directed), gamma 2, accessory subunit	1.26
20916	succinate-Coenzyme A ligase, ADP-forming, beta subunit	1.25
15494	hydroxy-delta-5-steroid dehydrogenase, 3 beta- and steroid delta-isomerase 3	1.25
15512	heat shock protein 2	1.25
12039	branched chain ketoacid dehydrogenase E1, alpha polypeptide	1.24
104910	expressed sequence AI132487	1.24
57423	ATP synthase, H+ transporting, mitochondrial F0 complex, subunit f, isoform 2	1.23
18975	polymerase (DNA directed), gamma	1.20
50529	mitchondrial ribosomal protein S7	1.20
69955	phenylalanine-tRNA synthetase 2 (mitochondrial)	1.18
53895	caseinolytic peptidase, ATP-dependent, proteolytic subunit homolog (E. coli)	1.16
269951	isocitrate dehydrogenase 2 (NADP+), mitochondrial	1.15
15488	hydroxysteroid (17-beta) dehydrogenase 4	0.87
29876	chloride intracellular channel 4 (mitochondrial)	0.85
71701	polyribonucleotide nucleotidyltransferase 1	0.84
30057	translocase of inner mitochondrial membrane 8 homolog b (yeast)	0.83
28295	DNA segment, Chr 10, Johns Hopkins University 81 expressed	0.83
14194	fumarate hydratase 1	0.83
66841	electron transferring flavoprotein, dehydrogenase	0.81
68463	mitochondrial ribosomal protein L14	0.81
16973	low density lipoprotein receptor-related protein 5	0.80
53333	translocase of outer mitochondrial membrane 40 homolog (yeast)	0.80
67270	DNA segment, Chr 10, ERATO Doi 322, expressed	0.53

Gene ID is the EntrezGene accession number that uniquely identifies the gene. Fold Change is the ratio of the mean expression of the indicated gene in diabetic mice to control mice.

The promoter regions of the DEGs were compared against the Genomatix database of experimentally validated TF modules (www.genomatix.de). Some TF modules were found to be significantly over-represented or under-represented in the regulated genes (Table 5). Results were sorted by the fold change in frequency of each module in the promoter region of these regulated genes compared with the frequency in all promoter regions in the mouse genome. Fold

change greater than 1 is indicative of over-representation and a fold change less than 1 under-representation. Modules that are over-represented in up-regulated genes are likely to have been up-regulated, and vice versa for modules over-represented in down-regulated genes.

Table 5 – Promoter Modules Significantly Altered in Regulated Metabolic and Mitochondrial Genes.

A – Upregulated Genes

Promoter Module	Fold Change in Frequency	p-value
NF1F_NR2F_01	3.88	0.001
SP1F_MYOD_01	2.44	0.03
STAT_ETSF_03	2.44	< 0.001
ETSF_ETSF_01	2.34	0.02
ETSF_SP1F_04	2.18	0.006
SORY_ETSF_01	1.70	< 0.001
ETSF_IRFF_01	1.18	< 0.001
IRFF_ETSF_01	1.13	0.001
NFKB_NKXH_01	0.82	< 0.001

B – Downregulated Genes

Promoter Module	Fold Change in Frequency	p-value
NFKB_AP1F_01	10.01	0.003
SP1F_EBOX_SP1F_01	7.16	0.002
EREF_SF1F_01	4.32	0.03
SP1F_SP1F_01	2.75	0.03
ETSF_SP1F_04	2.18	0.05
SORY_ETSF_01	2.12	0.002
NFKB_NKXH_01	1.53	< 0.001
ETSF_IRFF_01	0.94	0.03

Promoter modules are the experimentally characterized combination of TF binding sites found in the promoter region of the regulated genes. Fold change in frequency is the fold change in the percentage of genes with this promoter module in the regulated genes compared with all mouse promoters. p-value is the probability of finding this degree of change in frequency by chance, calculated using Fisher's Exact test.

Identifying Common TF Modules

Common transcription factors control the regulation of the genes regulated by both diabetes and Rosi. The promoter regions of the two gene groups were searched for conserved TF binding modules using the Genomatix FrameWorker tool. No modules were significantly enriched in the promoter region of genes up-regulated by diabetes and down-regulated by Rosi. Twenty-nine novel modules were enriched in the genes down-regulated by diabetes and up-regulated by Rosi ($p < 0.05$) (Table 6). Genes containing these modules were identified by screening the promoter region of all mouse genes. Gene Set Enrichment Analysis (GSEA) was used to test the hypothesis that these genes are up-regulated by Rosi by comparing gene expression levels between control and control + Rosi mice. The genes containing the SP1F_ZBPF or EGRF_EGRF modules were found to be significantly up-regulated by Rosi treatment ($p < 0.05$) (Fig. 3).

Table 6 – Top 5 Significantly Enriched and Regulated TF Binding Motifs.

TF Module	Frameworker p-value	GSEA p-value
SP1F_ZBPF	9.94E-04	1.50E-02
EGRF_EGRF	2.27E-03	3.07E-02
ZBPF_EGRF	2.16E-03	5.77E-02
ETSF_ETSF	7.77E-06	1.22E-01
ZBPF_SP1F_SP1F	7.81E-06	1.27E-01

FrameWorker p-values are the probability that the binding motif could be found in the promoter region of a set of genes by chance. The module search is performed repeatedly on randomly selected promoter regions to approximate the frequency of matching a promoter sequence by chance. This distribution is the basis for a Z-test to determine how likely it is that the genes were found by chance. GSEA p-values are the probability that a random gene set could show the same degree of directional regulation as was found in the query gene set.

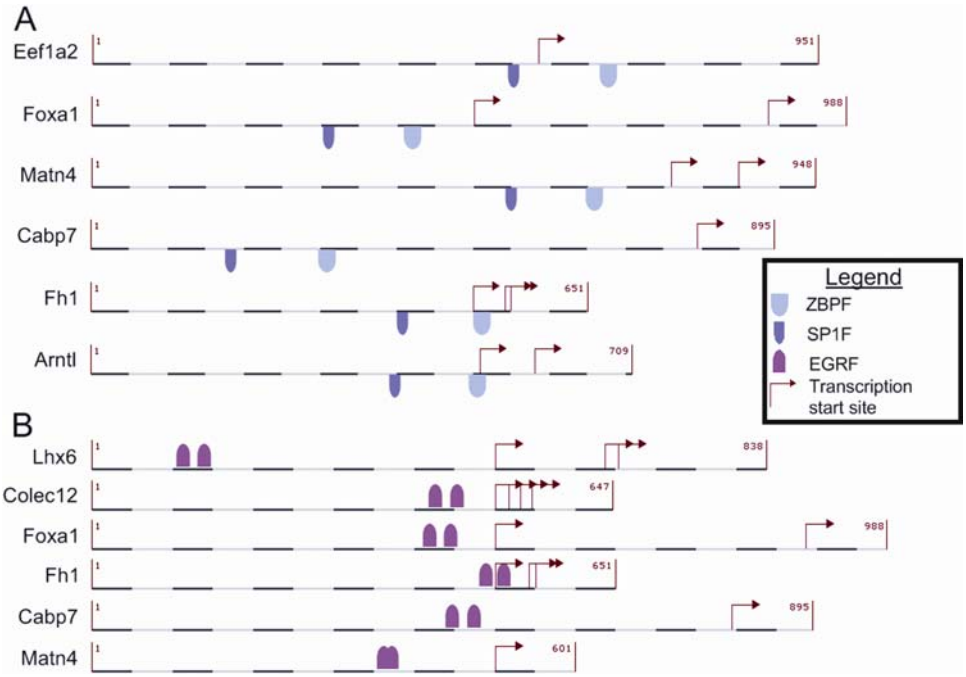

Fig. 3. Significant Promoter Modules. The conserved binding motifs found to be significant by FrameWorker and GSEA. A) The SP1F_ZBPF motif, B) the EGRF_EGRF motif.

Summary

The current study evaluated DBA/2J-STZ mice and the effect of Rosi treatment on the development of DN. We found that 1) the DBA/2J-STZ mice developed DN, 2) Rosi treatment significantly improved thermal latency and reduced oxidative stress in the sciatic nerve and 3) two novel promoter modules were regulated by both diabetes and Rosi and are likely relevant to the development.

In order to determine whether the amelioration of DN observed is due to a reduction of diabetes-induced oxidative stress, biomarkers of oxidative damage were assayed in the sciatic nerve. Both dityrosine and HODE were significantly elevated in the DBA/2J-STZ mice, consistent with previous work showing that diabetes increases oxidized lipids (21, 22) and protein (23). Our findings are consistent with the oxidative stress model of DN (24), as thermal latency is highly correlated with increased levels of dityrosine and HODE. Treatment with Rosi reduced both biomarkers significantly, to levels near that of control animals. Because Rosi did not correct hyperglycemia but did reduce oxidative stress, we hypothesize that Rosi promotes anti-oxidant activity.

Common promoter elements among these functionally related, diabetes-altered genes could explain their regulation. The search for metabolic genes regulated by diabetes led to the identification of several well-characterized regulatory elements involved in hyperglycemia-induced changes in gene expression. The most highly up-regulated module, NF1F_NR2F_01, was first identified in the promoter region of pyruvate kinase L (Pklr) (25). The promoter is activated by increased dietary glucose in healthy mice and insulin in diabetic mice, resulting in an expression change of Pklr in the liver (26). High glucose levels in diabetic mice may result in high baseline activity for this module and lead to the observed increase in gene expression of its targets. Therefore, the activation of this module is likely an effect of diabetes, however, its status as a therapeutic target for DN has yet to be defined.

The SP1F_ZBPF binding site is a module that contains binding domains for a stimulating protein 1 (Sp1) family TF and a Krüppel-like zinc finger TF. The apparent regulation of this domain is consistent with studies showing that Sp1 is activated by insulin stimulated glucose metabolism (27) while Krüppel-like factors are associated with apoptosis, survival and neurite outgrowth (28). While no PPAR-gamma binding motif was found associated with this module, PPAR-gamma stimulates a similar promoter module of Sp1, SRE and double E-box in mouse adipocytes (29) independent of a specific DNA binding motif. Sp1 is an intermediate step in the PPAR-gamma induction of resistin (30) and hormone-sensitive lipase (31), while PPAR-gamma suppresses Sp1 expression in a lung carcinoma cell line (32). Similarly both TZD (33) and non-TZD (34) activation of PPAR-gamma induces Krüpple-like-factor 4 in colon cancer cells. Both of the TFs identified in this module have functional associations with diabetes, and both respond to PPAR-gamma activation. These separate lines of evidence support our contention that the SP1F_ZBPF module may constitute a novel therapeutic target in the treatment of DN.

The EGRF_EGRF motif is a double binding site for early growth factor 1 & 2 (Egr-1, Egr-2) and similar C2H2 zinc finger factors. A similar artificial motif was used to detect Egr-1 activity (35), lending plausibility to the functionality of this module. In the developing nervous system, Egr-2 mutations are associated with childhood demyelinating diseases (36), and Egr-1 plays a continuing role in the maintenance of the myelin sheath in the adult peripheral nervous system (37). In the present study, genes with this promoter module are down-regulated by diabetes and up-regulated by Rosi treatment. A non-TZD class of PPAR-gamma agonists, methylene-substituted diindolylmethanes, indirectly activate Egr-1 through a phosphatidylinositol 3-kinase (PI3K) dependent mechanism in prostate and colon cancer cell lines (38). Conversely, PPAR-gamma inhibits Egr-1 in carbon monoxide treated macrophages (39), lung tissue following ischema-reperfusion (40) and in response to spinal cord injury (41). While the direction of regulation varies by tissue type and insult, PPAR-gamma clearly affects the expression and activity of Egr-1, consistent with our experimental findings. Our experimental findings and known regulatory association indicate that the EGRF_EGRF module may also constitute a novel therapeutic target in the treatment of DN.

In conclusion, this study demonstrates that the DBA/2J-STZ mouse develops and maintains DN. DN is highly correlated with the oxidative stress present in the sciatic nerve, and both are reduced by Rosi treatment. Using a systems biology approach, we found significant changes in gene expression induced by diabetes and Rosi, and that two TF binding modules, SP1F_ZBPF and EGRF_EGRF, are likely involved. These modules constitute novel drug targets, and merit future study.

Plans for the Upcoming Year

We have embarked on 3 pathways. First, we will validate the TF binding modules described above are involved in the gene expression changes in diabetes. Of note, our Genomatix promoter search was limited to cis-acting transcriptional elements in order to reduce the scope of the searches performed. However, it is possible that regulatory elements more than 500 bp upstream (42) or located in an intron more than 100 bp downstream (43) of the TSS play a significant role in the transcription of these genes. If these promoter modules prove to be insufficiently specific in further experiments, it would be necessary to assess the activity of such trans-acting elements more carefully.

Secondly, we need to complete the microarray analyses and bioinformatics analyses for the BKSdbdb animals using the paradigm outlined above that we completed for the DBA-2J mice. This was suggested to us by the EAC, and as indicated in our response to the EAC, we are actively pursuing this with very interesting results.

Finally, we will pursue two new animal models to investigate our novel hypothesis that increased levels of plasma lipids and oxidative stress act in concert with glucose to produce injury

leading to diabetic neuropathy. Our goal is to establish the role of dyslipidemia and the relative contributions of dyslipidemia and hyperglycemia to the development of neuropathy in mouse models. The mice we have selected for this study were developed by Murielle Veniant-Ellison and co-workers at Amgen (can provide MTA upon request). They developed triple knockout (3 KO) mice that are deficient in either ApoE or in the low density lipoprotein receptor Ldlr and are both additionally lacking leptin (ob/ob) and apolipoprotein B-48. Both lines develop obesity, hyperinsulinemia, hyperlipidemia, hypertension, and atherosclerosis. However, only ApoE 3KO mice are hyperglycemic and glucose intolerant - they are more obese than Ldlr 3KO mice. By comparing neuropathy phenotypes and biochemical changes between these lines we will determine the contribution of dyslipidemia to the onset and progression of neuropathy. Our goal is to phenotype mice for the onset and progression of neuropathy over time and, at 6 months of age, perform terminal neuropathy phenotyping, including metabolic profiling of lipids and oxidative modifications in plasma, DRG, and sciatic nerve and explore the biochemical alterations in mitochondria, NAD(P)H oxidase, and the oxidative stress pathways. A plan for our work is presented in Table 7.

The mice will be maintained on the same chow as the original studies , the 22/5 Rodent Diet from Harlan Teklad (Indianapolis, IN), containing 22% protein, 5% fat, and 4.5% fiber. Mice will be assigned to groups of 12 mice each as follows: ApoE 3KO, Ldlr 3KO and C57BL/6 wt. These 3 groups will be maintained up to 24 wk age. Phenotyping will be performed according to the schedule in Table 7. Eight animals per group is powered to detect a 2 msec change in hind paw withdrawal and 2 m/sec change in motor nerve conduction velocity (44) so 12 animals per group should provide sufficient numbers to complete the study.

Table 7. Neuropathy Phenotyping Schedule for 3 KO Mice and Controls.

Evaluation	Week 4	Week 8	Week 12	Week 16	Week 20	Week 24
Weight	X	X	X	X	X	X
Glucose	X	X	X	X	X	X
HbA1C						X
Glucose Tolerance Test			X			X
Lipids, oxLDL, oxidative stress markers						X
Tail blood pressure	X		X			X
Thermal sensitivity testing	X	X	X	X		X
Nerve conductions			X			X
Von Frey mechanical sensation	X	X	X	X	X	X
Intraepidermal nerve fiber density & skin microvessel analysis						X
IHC markers						X
DRG TUNEL						X
Tissue Harvest						X

We are also investigating the role of dyslipidemia and neuropathy in two other animal models. For a type 1 model, we have treated the DBA2J mice with fenofibrate; initial data are presented in Table 8 and details will be available to the EAC in the next reporting period. For another type 2 model (other than the 3KO mice described above), we have crossed the ApoE knockout mice onto a db/db (leptin deficient) background. Our goal is to demonstrate that further perturbations in plasma lipids will compound the progression of diabetic neuropathy in these mice. We present preliminary data with small groups of these mice (Table 8). These animals underwent electrophysiological and behavioral phenotyping at 12 wk age . The groups are too small for statistical analysis, but we observe a trend to slower hind paw withdrawal and sciatic motor nerve

conduction velocity with loss of leptin expression ahead of the development of insulin resistance. Db+ mice do not develop diabetes, yet here we demonstrate a trend to increase neuropathy in ApoE-/- db+ compared to ApoE-/- wild type (ApoE wt) (Table 8).

Preliminary Milestones for 2009 and Beyond

Our milestones for 2009 are completion of the 2008 and 2009 goals. Specifically, we will confirm our informatics approach to identifying new promoter modules and specific transcription factors, pursue the experiments outlined for us by the EAC and continue to explore the role of dyslipidemia in neuropathy.

2. Collaboration:

Collaborations With Other AMDCC Groups: Brosius and Kretzler

Because we are searching for multi-organ mechanisms and treatments, the two promoter modules identified as being activated in the nerve as outlined above in our progress report were tested in mouse and human kidney. Gene expression studies were performed on glomeruli harvested from the DBA/2J mice used in the previous experiment and human kidney biopsies from type 2 diabetic patients treated with TZD. We received these data from our AMDCC collaborators, Drs. Brosius and Kretzler. The promoter modules were tested for functional relevance by comparing their prevalence in regulated genes compared with all genes. The custom promoters are significantly enriched in both Human and Mouse kidney (Table 8).

Table 8. Transcription Factor Modules Relevant to Multiple Tissues and Species.

Tissue	Module	p-value	FC
Mouse Kidney	EGRF_EGRF	4.77E-34	1.53
Mouse Kidney	SP1F_ZBPF	1.03E-20	1.75
Human Kidney	SP1F_ZBPF	5.71E-04	2.52
Mouse Nerve	SP1F_ZBPF	9.24E-04	2.59
Mouse Nerve	EGRF_EGRF	6.62E-03	1.72
Human Kidney	EGRF_EGRF	6.81E-03	1.66

Fisher's exact test p-values bonferroni corrected. Fold Change (FC) measured against promoter regions of all annotated genes in the relevant species.

Identification of Transcription Factors Modulating Gene Expression

After finding that the custom modules were significantly enriched in multiple tissues, we have begun the process of identifying the specific transcription factors likely binding to the motifs involved: SP1F, ZBPF and EGRF. The microarray data were re-examined for genes that bind the SP1F motif and are regulated by both diabetes and Rosi treatment across the three experimental conditions. The genes trans-acting transcription factor 3 (Sp3) and Kruppel-like factor 16 (KLF16) were identified as the most likely candidates for RT-PCR confirmation. Sp3 is an inhibitory transcription factor, and increased expression would be anticipated to cause decreased gene transcription, and vice versa. As predicted, Sp3 was up-regulated in diabetes and down-regulated by Rosi treatment. While this effect did not reach significance in the sciatic nerve ($p = 0.08$), our small sample size ($n = 4$) may have limited our ability to detect significant changes.

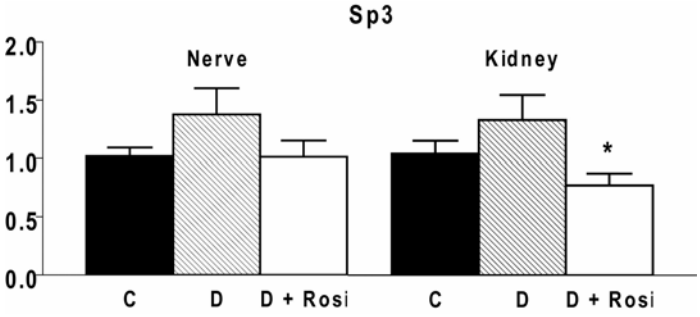

Fig. 4. RT-PCR Confirmation of Sp3 Expression Plotted as Fold Change v. Control. Expression measured using Tbp as a reference. C – Control, D – Diabetic, D + Rosi – Diabetic + Rosi. * $p < 0.05$.

Gene Expression in a Type 2 Model of DPN

In addition to the Type 1 mouse model used above, we have performed a microarray experiment analyzing the C57/BKS db/db mouse, a type 2 model of diabetes. These data are preliminary, are in response to the EAC comments and will be presented more fully in the next progress report (discussed in more detail below). There is only a minor overlap in the genes regulated, similar to the small overlap found between our type 1 nerve and kidney data (Fig. 5). This finding reinforces the necessity of a sophisticated, promoter and pathway oriented analysis to identify the common features between these disease processes and how they are affected by different drug treatments.

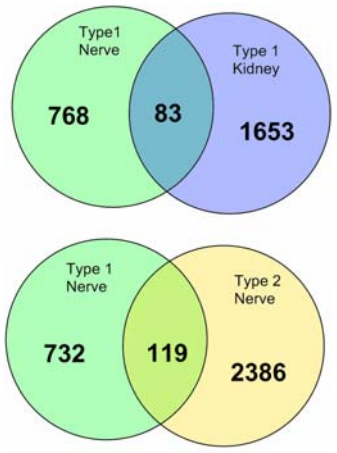

Fig. 5. Venn Diagram of Regulated Gene Overlap.

Collaborations with Other AMDCC Groups: Smithies and Abel

Smithies: We completed neuropathy phenotyping on the bradykinin/akita mice supplied by the Smithies laboratory via JAX. We do not see a neuropathy phenotype in these animals. We anticipate this is due in part to the fact the animals are the C57Bl6 background. We have reported that this strain, regardless of the superimposed transgene, is resistant to diabetic neuropathy when diabetes is induced using the AMDCC 5 day low dose STZ protocol.

Abel: We have begun two new collaborative efforts with the Abel laboratory. First, when the Abel laboratory has induced diabetes with STZ in a strain of mice that has not yet undergone neuropathy phenotyping, these mice are shipped to us to perform terminal phenotyping at 6 months of age (see CD1 data and Swiss Webster). We then return the tissues of interest to the Abel laboratory for their use. Table X represents neuropathy phenotyping of both Swiss Webster and CD1A strains. Secondly, the Abel laboratory is currently treating Swiss Webster mice, made diabetic with STZ, with netrin. Phenotyping of these animals yielded an interesting and reproducible difference in hind paw withdrawal thresholds with no change in sural or sciatic nerve conduction velocities. This would suggest that neurtrin is preserving small fiber function. We are currently analyzing the intraepidermal nerve fiber density of these animals to assess the small fiber anatomy.

Strain	Diabetes induction	Weight	Blood Glucose	Tail Flick	Hind Paw	Sciatic NCV	Sural NCV	IENF
CD-1 (Abel)	None	45.31 ± 0.46 *n = 10*	133.7 ± 1.77 *n = 10*	7.37 ± 0.11 *n = 10*	5.56 ± 0.14 *n = 8*	46.3 ± 0.77 *n = 10*	26.9 ± 0.26 *n = 10*	41.85 ± 0.38 *n = 9*
	STZ	34.16 ± 0.44 *n = 7*	583.71 ± 6.16 *n = 7*	9.44 ± 0.21 *n = 7*	8.66 ± 0.36 *n = 7*	47.57 ± 0.49 *n = 7*	22.14 ± 0.52 *n = 7*	37.51 ± 0.31 *n = 5*
Swiss Webster (Abel)	None	31.82 ± 0.73 *n = 8*	120.50 ± 2.35 *n = 8*	7.45 ± 0.13 *n = 8*	4.12 ± 0.04 *n = 8*	42.29 ± 0.72 *n= 7*	22.43 ± 0.20 *n = 7*	40.46 ± 1.16 *n = 5*
	STZ	29.04 ± 0.38 *n = 7*	(Over 400) *n = 7*	8.29 ± 0.12 *n = 7*	8.12 ± 0.37 *n = 7*	36.4 ± 1.30 *n = 5*	16.00 ± 0.32 *n = 5*	34.81 ± 0.60 *n = 6*
C57BL6 bradykinin -/- (Smithies)	akita +/-	27.51 ± 0.14 *n = 7*	159.29 ± 5.46 *n = 7*	2.61 ± 0.04 *n = 7*	3.57 ± 0.07 *n = 7*	35.29 ± 0.85 *n = 7*	17.43 ± 5.46 *n = 7*	
	akita +/+	23.38 ± 0.23 *n = 7*	449.57 ± 18.64 *n = 7*	3.2 ± 0.03 *n = 6*	3.60 ± 0.04 *n = 7*	32.86 ± 0.95 *n = 7*	17.14 ± 0.41 *n = 7*	
C57BLKS (EAC recommend)	db+	28.8 ± 0.18 *n = 10*	144.4 ± 3.11 *n= 10*	3.89 ± 0.08 *n= 10*	2.69 ± 0.04 *n= 10*	46.2 ± 0.18 *n= 10*	18.9 ± 0.26 *n= 10*	41.29 ± 0.20 *n = 8*
	db/db	51.23 ± 0.23 *n = 10*	454 ± 16.76 *n = 10*	6.04 ± 0.13 *n = 10*	3.50 ± 0.04 *n = 10*	23.0 ± 0.53 *n = 10*	13.4 ± 0.37 *n = 10*	25.50 ± 0.61 *n = 7*

Values are mean ± standard error

Strain	Diabetes induction	Treatment	Weight	Blood Glucose	Tail Flick	Hind Paw	Sciatic NCV	Sural NCV
C57BLKS (new aim)	db/+	ApoE+/-	25.09 ± 0.73 *n = 4*	155.75 ± 8.06 *n = 4*	4.94 ± 0.11 *n = 5*	2.86 ± 0.09 *n = 5*	36.14 ± 1.24 *n = 7*	12.67 ± 0.38 *n = 7*
	db/db		37.35 *n = 1*	598 *n = 1*	4.68 ± 0.16 *n = 3*	4.12 ± 0.24 *n = 4*	29.00 ± 1.95 *n = 4*	15.25 ± 0.69 *n = 4*
	db/+	ApoE-/-	30.08 *n = 1*	133 *n = 1*	4.65 ± 0.13 *n = 4*	2.91 ± 0.11 *n = 4*	39 ± 0.96 *n = 5*	14.60 ± 0.36 *n = 5*
	db/db				3.54 *n = 1*	2.95 *n = 1*	28.67 ± 1.17 *n = 3*	12.667 ± 0.38 *n = 3*
DBA/2 (new aim)	None	None	31.18 ± 0.79 *n = 2*	139.00 ± 12.02 *n = 2*	6.28 ± 0.47 *n = 2*	4.43 ± 0.82 *n = 2*	45.5 ± 1.77 *n = 2*	22.0 ± 0.71 *n = 2*
	STZ							
	None	Fenofibrate	26.29 ± 1.2 *n = 2*	114.00 ± 6.37 *n = 2*	5.95 ± 0.35 *n = 2*	5.63 ± 0.89 *n = 2*	47.0 ± 0.71 *n = 2*	21.5 ± 1.06 *n = 2*
	STZ		15.81 ± 0.21 *n = 2*	501.00 ± 14.14 *n = 2*	7.54 ± 0.05 *n = 2*	10.61 ± 0.74 *n = 2*	36.6 ± 1.06 *n = 2*	15.5 ± 1.06 *n = 2*
Swiss Webster (Abel)	None	PBS	39.23 ± 0.48 *n = 10*	140.30 ± 2.01 *n = 10*	7.08 ± 0.11 *n = 10*	4.42 ± 0.06 *n = 10*	42.60 ± 0.90 *n = 10*	21.4 ± 0.29 *n = 10*
	STZ		29.48 ± 0.72 *n = 5*	565.5 ± 9.98 *n = 4*	8.30 ± 0.38 *n = 4*	7.03 ± 0.27 *n = 4*	31.40 ± 1.57 *n = 5*	14.80 ± 0.43 *n = 5*
	None	Netrin	39.13 ± 0.57 *n = 9*	146.67 ± 2.34 *n = 9*	7.01 ± 0.7 *n = 9*	4.24 ± 0.07 *n = 9*	46.25 ± 1.15 *n = 8*	19.38 ± 0.40 *n = 8*
	STZ		30.89 ± 0.37 *n = 6*	583.75 ± 15.91 *n = 4*	7.67 ± 0.37 *n = 4*	4.64 ± 0.24 *n = 4*	29.60 ± 1.17 *n = 5*	14.50 ± 0.25 *n = 6*

Values are mean ± standard error

JAX Laboratory Update

13 N4 BKSB6-Sod2tm1Shs heterozygous mice were identified for SNP typing. Animals tested ranged from 3-6 segregating SNP markers out of 105. 4 males and 2 females with 3–5 segregating markers were selected for generating N5 progeny to the BKS-Leprdb. This will most likely be the last backcross for this stock. The next generation JAX will start to intercross the mice to get mice that are homozygous for the Sod2 allele that will be needed to mate to Stock No. 7219 -- BKS.B6-Tg(Nes-cre)1Kln/J.

Numbers 184 and 163 are identified by JAX as the favorite for the most recent round of testing. Both have 4 segregating SNP markers. 163 has 1 expected segregating marker on Chr.

4 in the region of the Lepr<db> allele. It also has 3 segregating markers on Chr. 17 in the region of SOD2<Floxed> allele. Male 184 has 1 expected segregating marker on Chr. 4, a marker on Chr. 15 and 2 markers on Chr. 17 around the SOD2<Floxed> allele. This male has the shortest congenic interval of any of the animals. If JAX can "clean up" Chr. 15 in his progeny they will use his progeny to advance our project. JAX also likes 164, 168, 167, 171 and 173. These animals only have segregating markers on Chr. 4 around the Lepr<db> allele and on Chr. 17 around the SOD2<floxed> allele. However, these animals have a much longer congenic interval on Chr. 17 which is less appealing to JAX. These 7 animals will be set up into mating with BKS-db this week.

3. <u>Address Previous EAC Comments</u>:

EAC comments are in italics and are addressed in the order presented.

1. *Must work closely with JAX to determine appropriate strain controls. This discussion should be open to a refinement of the proposed model.*
   We fully agree with the EAC and are working with JAX as outlined above.

2. *Generation of the Nestin Cre may be helpful to nephropathology projects. Nestin is highly expressed in adult podocytes.*
   The Nestin-Cre animals are now available on the BKLS background and we will be happy to distribute them to any interested investigator.

3. *Continued efforts to work with broader community to establish validation criteria are lauded. Since Dr. Feldman's is the only neuropathy group in the consortium, this is certainly the best way forward.*
   With the support of the AMDCC and the JDRF, we are holding a satellite symposium at the Neurodiab meeting on September 2-3 in Orvieto, Italy. Our goal is to establish a set of criteria for phenotyping murine models of diabetic neuropathy that are broadly accepted by the academic community.

4. *The SOD data are very interesting and getting SOD onto BKS-db/db should have a high priority. Given the interesting nephropathy data - maybe even better onto BKS-db/db,eNOS-/+?*
   This is occurring via JAX (cell type specific). We are generating the BKS-db/db ApoE -/- animals but are not yet generating the eNOS double transgenic, due to constraint of time/funds. The idea is very interesting.

5. *Oxidative stress measures and microarray experiments are planned on the B6/STZ and BKS/db combinations. Would it be worthwhile to carry out these experiments on the BKS background to begin with since this seems to be one of the better backgrounds for complications? Or include BKS/STZ in the experiments to be able to compare the two diabetes protocols (in B6 STZ is inducing massive changes in mitochondrial proteins).*
   At the EAC's suggestion we elected to begin our work on the BKS background and agree this is the best approach. We completed and published behavioral and electrophysiological phenotyping of the BKS dbdb mice (18), and are continuing to expand our approach and numbers (Table 8).

   We have just completed the measures of oxidative stress, as suggested by the EAC (Fig. 6).

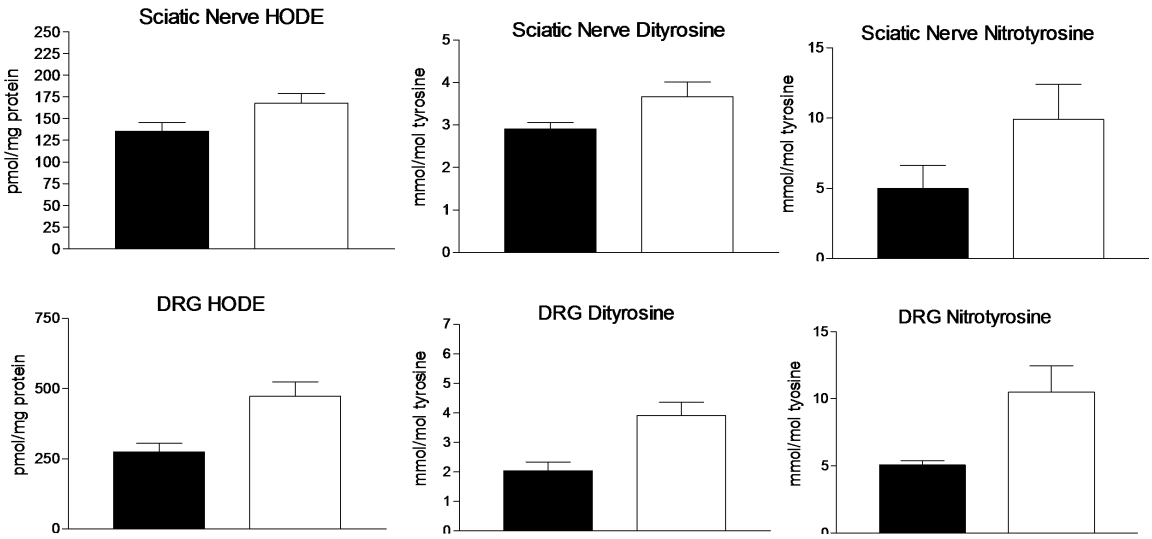

Fig. 6 Oxidative stress measures from 24 wk old BKS-db$^+$ (black bars) and BKS-db/db (open bars) mice (data processed as outlined in Fig. 1).

The microarray analysis is preliminary, but reveals interesting differences between type 1 and type 2 nerve (Fig. 5) and nerve and dorsal root ganglia neurons. These data will be fully reported in our next report.

Publications (names in bold are AMDCC members):

1. Sullivan KA, Hayes JM, Wiggin TD, Backus C, Oh S, Lentz SI, **Brosius F**, **Feldman EL**. Mouse models of diabetic neuropathy. *Neurobiology of Disease*, 28, 276-285, 2007.

2. Vincent AM, Russell JW, Sullivan KA, Backus C, Hayes JM, McLean LL, **Feldman E**L. SOD2 protects neurons from injury in cell culture and animal models of diabetic neuropathy. *Experimental Neurology*, 208, 216-227, 2007.

3. Vincent AM and **Feldman, EL**. Can drug screening lead to candidate therapies for testing in diabetic neuropathy? *Antioxidants & Redox Signaling*, 10, 387-394, 2008.

4. **Feldman E**L. Diabetic neuropathy. *Current Drug Targets*, 9, 1-2, 2008.

5. Sullivan KA, Lentz SI, Roberts JL Jr, **Feldman EL**. Criteria for creating and assessing mouse models of diabetic neuropathy. *Current Drug Targets*, 9, 3-13, 2008.

6. Vincent AM, Edwards JL, Sadidi M, **Feldman E**L. The antioxidant response as a drug target in diabetic neuropathy. *Current Drug Targets*, 9, 94-100, 2008.

7. Vincent AM, Sakowski SA, Schuyler A, **Feldman EL**. Strategic approaches to developing drug treatments for ALS. *Drug Discover Today*, 13, 67-72, 2008.

8. **Feldman E**L, Cornblath DR, Porter J, Dworkin R, Scherer S. National Institute of Neurological Disorders and Stroke (NINDS) Meeting Summary: Advances in understanding and treating neuropathy, October 24-25, 2006, Bethesda, Maryland. *Journal of the Peripheral Nervous System*, 13, 1-6, 2008.

9. Russell JW, Berent-Spillson A, Vincent AM, Freimann CL, Sullivan KA, **Feldman EL**. Oxidative injury and neuropathy in diabetes and impaired glucose tolerance. *Neurobiology of Disease*, *Neurobiology of Disease*, 30, 420-429, 2008.

10. Zhang H, Saha J, Schin M, Byun J, **Kretzler M, Feldman EL**, Weil DA, Pennathur S, **Brosius III FC**. Rosiglitazone prevents renal and plasma markers of oxidative injury and reverses urinary metabolite abnormalities in the amelioration of diabetic nephropathy. *The American Journal of Physiology – Renal Physiology*, in press.

11. Qian Y, **Feldman E,** Pennathur S**, Kretzler M, Brosius III FC**. From fibrosis to sclerosis. Mechanisms of glomerulosclerosis in diabetic nephropathy. *Diabetes*, in press.

12. **Kern TS**, Berkowitz BA, **Feldman EL.** National Institute of Diabetes and Digestive and Kidney Diseases (NIDDK) meeting summary. Advances toward measuring diabetic retinopathy and neuropathy: From the bench to the clinic and back again (April 4-5, 2007, Baltimore, Maryland). *Journal of Diabetes Complications*, in press.

13. Muller KA, Ryals JM, **Feldman EL**, Wright DE. Abnormal muscle spindle innervation and large-fiber neuropathy in diabetic mice. *Diabetes*, in press.

Literature Cited

1. Bhatia V, Viswanathan P. Insulin resistance and PPAR insulin sensitizers. Curr Opin Investig Drugs 2006;7:891-897.
2. Chang AY, Wyse BM, Gilchrist BJ, Peterson T, Diani AR. Ciglitazone, a new hypoglycemic agent. I. Studies in ob/ob and db/db mice, diabetic Chinese hamsters, and normal and streptozotocin-diabetic rats. Diabetes 1983;32:830-838.
3. Chang AY, Wyse BM, Gilchrist BJ. Ciglitazone, a new hypoglycemic agent. II. Effect on glucose and lipid metabolisms and insulin binding in the adipose tissue of C57BL/6J-ob/ob and -+/? mice. Diabetes 1983;32:839-845.
4. Fujita T, Sugiyama Y, Taketomi S, et al. Reduction of insulin resistance in obese and/or diabetic animals by 5-[4-(1-methylcyclohexylmethoxy)benzyl]-thiazolidine-2,4-dione (ADD-3878, U-63,287, ciglitazone), a new antidiabetic agent. Diabetes 1983;32:804-810.
5. Vasudevan AR, Balasubramanyam A. Thiazolidinediones: a review of their mechanisms of insulin sensitization, therapeutic potential, clinical efficacy, and tolerability. Diabetes Technol Ther 2004;6:850-863.
6. Yamagishi SI, Ogasawara S, Mizukami H, et al. Correction of protein kinase C activity and macrophage migration in peripheral nerve by pioglitazone, peroxisome proliferator activated-gamma-ligand, in insulin-deficient diabetic rats. J Neurochem 2007.
7. Desvergne B, Wahli W. Peroxisome proliferator-activated receptors: nuclear control of metabolism. Endocr Rev 1999;20:649-688.
8. Sears DD, Hsiao A, Ofrecio JM, Chapman J, He W, Olefsky JM. Selective modulation of promoter recruitment and transcriptional activity of PPARgamma. Biochem Biophys Res Commun 2007;364:515-521.
9. Dumasia R, Eagle KA, Kline-Rogers E, May N, Cho L, Mukherjee D. Role of PPAR-gamma agonist thiazolidinediones in treatment of pre-diabetic and diabetic individuals: a cardiovascular perspective. Curr Drug Targets Cardiovasc Haematol Disord 2005;5:377-386.
10. Giannini S, Serio M, Galli A. Pleiotropic effects of thiazolidinediones: taking a look beyond antidiabetic activity. J Endocrinol.Invest 2004;27:982-991.

11. Ghosh S, Patel N, Rahn D, et al. The thiazolidinedione pioglitazone alters mitochondrial function in human neuron-like cells. Mol Pharmacol 2007;71:1695-1702.
12. Hwang J, Kleinhenz DJ, Rupnow HL, et al. The PPARgamma ligand, rosiglitazone, reduces vascular oxidative stress and NADPH oxidase expression in diabetic mice. Vascul Pharmacol 2007;46:456-462.
13. Qiang X, Satoh J, Sagara M, et al. Inhibitory effect of troglitazone on diabetic neuropathy in streptozotocin-induced diabetic rats. Diabetologia 1998;41:1321-1326.
14. Nagasaka Y, Kaku K, Nakamura K, Kaneko T. The new oral hypoglycemic agent, CS-045, inhibits the lipid peroxidation of human plasma low density lipoprotein in vitro. Biochem Pharmacol 1995;50:1109-1111.
15. Deeg MA, Buse JB, Goldberg RB, et al. Pioglitazone and rosiglitazone have different effects on serum lipoprotein particle concentrations and sizes in patients with type 2 diabetes and dyslipidemia. Diabetes Care 2007;30:2458-2464.
16. Singh S, Loke YK, Furberg CD. Long-term risk of cardiovascular events with rosiglitazone: a meta-analysis. Jama 2007;298:1189-1195.
17. Faich GA, Moseley RH. Troglitazone (Rezulin) and hepatic injury. Pharmacoepidemiol Drug Saf 2001;10:537-547.
18. Sullivan KA, Hayes JM, Wiggin TD, et al. Mouse models of diabetic neuropathy. Neurobiol Dis 2007;28:276-285.
19. Vincent AM, Russell JW, Sullivan KA, et al. SOD2 protects neurons from injury in cell culture and animal models of diabetic neuropathy. Exp Neurol 2007;208:216-227.
20. Baldi P, Long AD. A Bayesian framework for the analysis of microarray expression data: regularized t -test and statistical inferences of gene changes. Bioinformatics 2001;17:509-519.
21. Saini AK, Kumar HSA, Sharma SS. Preventive and curative effect of edaravone on nerve functions and oxidative stress in experimental diabetic neuropathy. Eur J Pharmacol 2007;568:164-172.
22. Kumar A, Kaundal RK, Iyer S, Sharma SS. Effects of resveratrol on nerve functions, oxidative stress and DNA fragmentation in experimental diabetic neuropathy. Life Sciences 2007;80:1236-1244.
23. Ueno Y, Horio F, Uchida K, et al. Increase in oxidative stress in kidneys of diabetic Akita mice. Biosci Biotechnol Biochem 2002;66:869-872.
24. Vincent AM, Russell JW, Low P, Feldman EL. Oxidative stress in the pathogenesis of diabetic neuropathy. Endocr Rev 2004;25:612-628.
25. Tremp GL, Boquet D, Ripoche MA, et al. Expression of the rat L-type pyruvate kinase gene from its dual erythroid- and liver-specific promoter in transgenic mice. J Biol Chem 1989;264:19904-19910.
26. Yamada K, Noguchi T, Miyazaki J, et al. Tissue-specific expression of rat pyruvate kinase L/chloramphenicol acetyltransferase fusion gene in transgenic mice and its regulation by diet and insulin. Biochem Biophys Res Commun 1990;171:243-249.
27. Moreno-Aliaga MJ, Swarbrick MM, Lorente-Cebrian S, Stanhope KL, Havel PJ, Martinez JA. Sp1-mediated transcription is involved in the induction of leptin by insulin-stimulated glucose metabolism. J Mol Endocrinol 2007;38:537-546.
28. Kaczynski J, Cook T, Urrutia R. Sp1- and Kruppel-like transcription factors. Genome Biol 2003;4:206.
29. Medvedev AV, Snedden SK, Raimbault S, Ricquier D, Collins S. Transcriptional regulation of the mouse uncoupling protein-2 gene. Double E-box motif is required for peroxisome proliferator-activated receptor-gamma-dependent activation. J Biol Chem 2001;276:10817-10823.

30. Chung SS, Choi HH, Cho YM, Lee HK, Park KS. Sp1 mediates repression of the resistin gene by PPARgamma agonists in 3T3-L1 adipocytes. Biochem Biophys Res Commun 2006;348:253-258.
31. Deng T, Shan S, Li PP, et al. Peroxisome proliferator-activated receptor-gamma transcriptionally up-regulates hormone-sensitive lipase via the involvement of specificity protein-1. Endocrinology 2006;147:875-884.
32. Han S, Ritzenthaler JD, Rivera HN, Roman J. Peroxisome proliferator-activated receptor-gamma ligands suppress fibronectin gene expression in human lung carcinoma cells: involvement of both CRE and Sp1. Am J Physiol Lung Cell Mol Physiol 2005;289:L419-428.
33. Drori S, Girnun GD, Tou L, et al. Hic-5 regulates an epithelial program mediated by PPARgamma. Genes Dev 2005;19:362-375.
34. Chintharlapalli S, Papineni S, Jutooru I, McAlees A, Safe S. Structure-dependent activity of glycyrrhetinic acid derivatives as peroxisome proliferator-activated receptor {gamma} agonists in colon cancer cells. Mol Cancer Ther 2007;6:1588-1598.
35. Cibelli G, Policastro V, Rossler OG, Thiel G. Nitric oxide-induced programmed cell death in human neuroblastoma cells is accompanied by the synthesis of Egr-1, a zinc finger transcription factor. J Neurosci Res 2002;67:450-460.
36. Berger P, Niemann A, Suter U. Schwann cells and the pathogenesis of inherited motor and sensory neuropathies (Charcot-Marie-Tooth disease). Glia 2006;54:243-257.
37. Decker L, Desmarquet-Trin-Dinh C, Taillebourg E, Ghislain J, Vallat JM, Charnay P. Peripheral myelin maintenance is a dynamic process requiring constant Krox20 expression. J Neurosci 2006;26:9771-9779.
38. Chintharlapalli S, Papineni S, Baek SJ, Liu S, Safe S. 1,1-Bis(3'-indolyl)-1-(p-substitutedphenyl)methanes are peroxisome proliferator-activated receptor gamma agonists but decrease HCT-116 colon cancer cell survival through receptor-independent activation of early growth response-1 and nonsteroidal anti-inflammatory drug-activated gene-1. Mol Pharmacol 2005;68:1782-1792.
39. Bilban M, Bach FH, Otterbein SL, et al. Carbon monoxide orchestrates a protective response through PPARgamma. Immunity 2006;24:601-610.
40. Okada M, Yan SF, Pinsky DJ. Peroxisome proliferator-activated receptor-gamma (PPAR-gamma) activation suppresses ischemic induction of Egr-1 and its inflammatory gene targets. Faseb J 2002;16:1861-1868.
41. Park SW, Yi JH, Miranpuri G, et al. Thiazolidinedione class of peroxisome proliferator-activated receptor gamma agonists prevents neuronal damage, motor dysfunction, myelin loss, neuropathic pain, and inflammation after spinal cord injury in adult rats. J Pharmacol Exp Ther 2007;320:1002-1012.
42. Thellmann M, Hatzold J, Conradt B. The Snail-like CES-1 protein of C. elegans can block the expression of the BH3-only cell-death activator gene egl-1 by antagonizing the function of bHLH proteins. Development 2003;130:4057-4071.
43. Nam S, Jin YH, Li QL, et al. Expression pattern, regulation, and biological role of runt domain transcription factor, run, in Caenorhabditis elegans. Mol Cell Biol 2002;22:547-554.
44. Sullivan KA, Lentz SI, Roberts JL, Jr., Feldman EL. Criteria for creating and assessing mouse models of diabetic neuropathy. Curr Drug Targets 2008;9:3-13.